The Journal of Energy: Engineering & Management
Vol. 12, No. 4, Winter 2023, P. 18-29
Research Article

Complete Load Compensation in a Distribution Network with a Single-Stage PV Grid Interface Converter

Hadi Afkar[1]*, Mostafa Esmaeeli[2]

[1] Department of Electrical Engineering, Technical and Vocational University (TVU), Tehran, Iran
h-afkar@tvu.ac.ir
[2] Faculty of Computer and Industrial Engineering, Birjand University of Technology, Birjand, Iran
esmaeeli@birjandut.ac.ir

Accepted: 12/11/2022 **Received:** 22/02/2023

Abstract
Recent promotions in renewable energy technology along with an increasing demand and the need for clean and cheap energy have led to an increasing trend towards distributed generation resources, especially solar cells, in distribution networks. Moreover, with the rapid development of electronic devices such as computers, televisions, and mobile phone chargers in the consumer sector and the use of power electronic devices such as converters in the industrial sector, the power quality of distribution networks has been seriously threatened. Therefore, it is very important to consider load compensation in distribution networks. In this paper, the use of a PV-grid interface converter for complete load compensation in a four-wire, three-phase distribution network is proposed. The proposed converter consists of a single-stage DC/AC inverter to connect solar cells to the grid. Maximum power point tracking of solar cells and injection of this power into the grid along with complete load compensation are done by the proposed DC/AC inverter. To achieve these aims, a new control strategy is proposed. Simulations wer performed in MATLAB/SIMULINK to evaluate the performance of the proposed structure and control strategy for the PV-grid interface converter. The simulation results for a four-wire, three-phase distribution system indicated complete nonlinear load compensation, reactive power compensation, load current harmonic elimination, and maximum PV power injection into the grid.

Keywords: PV-grid interface converter, complete load compensation, four-wire three-phase distribution network.

* Corresponding author
doi: 10.22052/JEEM.2023.113686

1. Introduction

More demands for electricity has increased the number of sensitive loads that require high-quality power as well as better a network performance. Additionally, the environmental pollution has been a serious issue due to an ever-increasing use of fossil fuels. These issues can be addressed by utilizing distributed generation (DG) systems [1-4]. Among distributed generation sources, the use of photovoltaics (PV) has more competitive advantages due to its inexhaustibility, availability, and pollution-free operation. For example, with a proper placement of PV panels, they can be used practically everywhere [5]. The main interface for connecting PV to the grid is power electronic converters.

Moreover, the use of more electronic power converters by residential, industrial, and commercial customers has led to the higher levels of reactive power and non-sinusoidal current in the grid. Therefore, the distortion due to the larger number of electronic power converters affects adjacent loads. The growth of nonlinear loads has imposed a serious challenge for providing power quality in microgrids and distribution networks [6]. These loads are increasingly important since they constitute more than 40% of the total electrical loads [7]. One of the most important concerns of power quality in distribution networks is current harmonics [8]. Besides, unlike three-phase, three-wire distribution networks, the power quality in three-phase, four-wire distribution networks is affected by an undesirable factor, i.e., neutral current. In distribution systems, unbalanced loads adversely affect generators and transformers. Moreover, the high current flow through the neutral line causes more serious issues of harmonics and reactive power. The compensation of neutral current is, thus, a very important measure in improving the power quality of a three-phase, four-wire distribution system. The injection of unbalanced current and reactive power has a distorting effect and reduces the power quality of distribution systems. Therefore, nonlinear load compensation and load balancing are chief problems in a modern distribution system. Low power quality in the power system can result in higher losses, in interference with telecommunication systems, and in annoying noises caused by vibrational torque in electrical machines [8-11].

THD current mitigation from nonlinear loads is frequently achieved by employing passive filters (PFs), active power filters (APFs), and hybrid APFs [12]. These solutions use additional tools (PFs, APFs, etc.) to compensate for non-linear loads in the grid. In order to compensate for loads, the remaining capacity of grid interface PV inverters can be used, especially in conditions of low solar irradiance. The auxiliary functions can be carried out by changing the control strategy of the inverter. PV inverters with auxiliary functions (or Multi-functional inverters) such as reactive power compensation, harmonics filtering capability, and load imbalance compensation are good proposition for grid-connected PVs because of an increase in nonlinear loads and an integration of PVs into the power grid. Multi-functional inverters have been used in PVs to achieve a cost-effective grid interface. Electronic power converters can play two roles in power grids; they can potentially alleviate power quality issues and serve as grid interfaces. Under these conditions, multi-functional inverters at the point of common coupling (PCC) can instantaneously enhance the power quality. Therefore, the space required by the system and the investment costs are reduced [13,14].

Auxiliary functions can include one or more types of power quality issues. However, among the studies, local nonlinear load current harmonic filtering and reactive power compensation are the most targeted [15-18]. Multi-functional PV grid interface converters are classified into the single-stage and the two-stage. In general, the higher number of stages decreases the efficiency of a grid interface converter. A two-stage grid interface converter consists of a DC/DC stage and a DC/AC stage. The DC/DC stage is usually used to realize maximum power point tracking (MPPT), whereas the DC/AC stage is used to control the power and current injected into the utility grid. A single-stage grid interface converter just has the DC/AC stage, which must complete all the functionalities of a two-stage one. A single-stage grid interface converter uses few electronic components and has smaller bulk, higher efficiency, lower cost, and higher reliability. On the contrary, the two-stage grid interface converter offers advantages such as a flexible control, but it has lower reliability, higher cost, and lower efficiency. Therefore, single-stage PV grid interface converters are commonly preferred in utility-scale applications [19-20].

The performance of the converter depends on the control strategy. Moreover, the control strategy is very important in achieving an optimal response of the system and realizing desirable goals according to the general performance. Various control strategies have been used in Multi-functional PV grid interface converters to improve grid power quality. Available strategies are based on either time or frequency domain analyses. In the frequency domain, the discrete Fourier transform algorithm is an approach with high complexity and poor dynamic response. Consequently, time domain-based strategies have been used more commonly. Among control strategies, instantaneous power theory in order has a straightforward physical meaning to identify and compensate for the reactive current and load harmonic, and its implementation in digital signal processors (DSPs) is easy [15-22]. In various studies, a single-stage PV grid interface converter has been used less for complete load compensation [21,22].

In this paper, a single-stage PV grid interface converter with a modified single-phase instantaneous power control strategy is proposed to compensate for the load (current harmonics, reactive power, unbalancing, and neutral current) in a four-wire, three-phase distribution network. The proposed converter uses only one DC/AC inverter to connect the PV system to the grid. Using the proposed control strategy, this DC/AC inverter performs maximum power point tracking (MPPT) along

with load compensation and injection of maximum PV power into the grid. The advantages of the proposed structure and its control strategy consists of a reduction in equipment costs, compared with two-stage structures, and its practical implement ability. In brief, the main contributions of this study could be listed as follows:

- A single-stage PV grid interface converter which uses a modified single-phase instantaneous power control strategy is proposed.
- The proposed structure and control strategy provide complete load compensation for unbalanced and nonlinear loads in three-phase, four-wire distribution systems.
- The realized complete load compensation includes load balancing on the grid side, neutral current elimination in the grid due to unbalanced loads, compensating load reactive power, enhancing network capacity, and reducing harmonic current generated by nonlinear loads in the grid.
- Ii injects maximum PV generation into the grid and load along with complete load compensation.

Accordingly, the organization of the paper is as follows.: the system structure is explained in section two. Section three presents a proposed control strategy. Section four presents MATLAB/SIMULINK simulation results. Finally, concluding remarks are presented in Section five.

2. System Configuration

The proposed system is shown in Fig. 1(a). This system connects PV modules to the grid via a single DC/AC converter in parallel with non-linear and unbalanced loads.

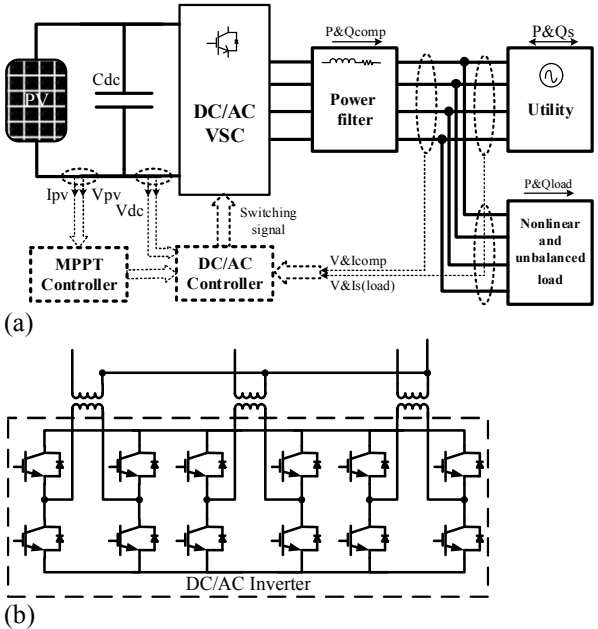

Fig. 1: (a) System structure and (b) DC/AC inverter

The DC/AC converter is responsible for DC voltage control, maximum power point tracking, power control, current injection into the network, and load compensation. Fig. 1(b) shows the structure of the converter, which uses three single-phase voltage source inverters (VSIs). The use of three single-phase VSIs allows load balancing. As another advantage of using VSIs, the system can be controlled either as three individual single-phase units or a single three-phase unit. Considering that one aims of the paper is load balancing while the maximum PV power are transferred to the grid, this necessitates the current of each phase should be controlled independently. Using the structure of three single-phase H bridges makes this function easily possible. In this situation, the voltage of each phase is the maximum H bridge voltage. Consequently, the inverter capacity is reduced due to a reduction in the DC link voltage (divided by √3) [21]. The important issue in single-stage grid interface inverters is that the level of PV voltage and grid voltage must be the same. Using the inverter shown in Fig. 1 (b), the proposed converter can be used in a single stage. Each of the VSIs is connected to the grid using a single-phase transformer, which isolates the grid from the converter and allows the connection of the converter to three-phase four-wire networks. To filter out the high-frequency current harmonics, a passive filter is employed in series with the DC/AC inverter.

3. Control strategy

In this paper, the grid-connected mode is considered to control the proposed converter. The inverter and load are in parallel. The control strategy of the converter has the following objectives: MPPT for the PV system, load compensation for power quality improvement, and the injection of PV power into the grid and load. In this situation, the major part of PV generation is dedicated to the grid and load, while the power quality on the grid side is also improved. When PV generation exceeds the energy consumed by the load, extra power is injected into the grid; otherwise, the load are supplied through the both of PV unit and grid.

The controller compensates for load and injects the PV power into the grid. The DC–AC converter simultaneously injects the PV power into the grid and loads with load compensation and power quality improvement on the grid side. To achieve these goals, the modified single-phase instantaneous power theory is used in the control strategy. In the present study, this method is generalized to control single-stage PV-grid interface inverters.

According to the single-phase instantaneous power theory, single-phase and two-phase systems are related with 90° leading or lagging. Moreover, a three-phase system can be defined by three individual two-phase systems. A two-phase system can be represented by the stationary frame α-β. Accordingly, actual currents and voltages are the α-axis quantities, while 90° leading or lagging voltage current is the β-axis quantities [9]. In the present study, the instantaneous power theory is the basis of control objectives, and the controlling strategy is generalized for single-stage PV-grid interface inverters operating in the grid-connected mode.

When the voltage of each phase is balanced, according to the single-phase p-q theory, one obtains:

Currents and voltages of phase in the α-β frame:

$$\begin{bmatrix} i_{La\_\alpha} \\ i_{La\_\beta} \end{bmatrix} = \begin{bmatrix} i_{La}(\omega t + \varphi_l) \\ i_{La}\left(\omega t + \varphi_l + \frac{\pi}{2}\right) \end{bmatrix} \quad (1)$$

$$\begin{bmatrix} V_{La\_\alpha} \\ V_{La\_\beta} \end{bmatrix} = \begin{bmatrix} V_{La}(\omega t) \\ V_{La}\left(\omega t + \frac{\pi}{2}\right) \end{bmatrix} = \begin{bmatrix} V_{lm}\sin(\omega t) \\ V_{lm}\cos(\omega t) \end{bmatrix} \quad (2)$$

Where i_{La} and V_{La} are the load current and voltage of phase a, i_{La_α}, i_{La_β} and V_{La_α}, V_{La_β} are the load currents and voltages of phase a in the α-β frame respectively.

Currents and voltages of phases b and c in the α-β frame:

$$\begin{bmatrix} i_{Lb,c\_\alpha} \\ i_{Lb,c\_\beta} \end{bmatrix} = \begin{bmatrix} i_{Lb,c}(\omega t + \varphi_l) \\ i_{Lb,c}\left(\omega t + \varphi_l + \frac{\pi}{2}\right) \end{bmatrix} \quad (3)$$

$$\begin{bmatrix} V_{Lb,c\_\alpha} \\ V_{Lb,c\_\beta} \end{bmatrix} = \begin{bmatrix} V_{Lb,c}(\omega t) \\ V_{Lb,c}\left(\omega t + \frac{\pi}{2}\right) \end{bmatrix} = \begin{bmatrix} V_{lm}\sin(\omega t \mp 120) \\ V_{lm}\cos(\omega t \mp 120) \end{bmatrix} \quad (4)$$

Where $i_{Lb,c}$ and $V_{Lb.c}$ are load currents and voltages of phase b and c, i_{Lb,c_α}, i_{Lb,c_β} and V_{Lb,c_α}, V_{Lb,c_β} are the load currents and voltages of phase b and c in the α-β frame respectively.

According to the p-q theory for balanced three-phase systems, instantaneous reactive and active powers are given below:

$$q_{L,abc} = V_{L,abc_\alpha}.i_{L,abc_\beta} - V_{L,abc_\beta}.i_{L,abc_\alpha} \quad (5)$$

and

$$p_{L,abc} = V_{L,abc_\alpha}.i_{L,abc_\alpha} + V_{L,abc_\beta}.i_{L,abc_\beta} \quad (6)$$

$p_{L,abc}$ and $q_{L,abc}$ are the three-phase instantaneous active and reactive powers of the load.

Therefore, according to the definition of three-phase power systems in the single-phase p-q theory, reactive and active powers can be obtained for each phase as follows:

$$\begin{bmatrix} p_{La,b,c} \\ q_{La,b,c} \end{bmatrix} = \begin{bmatrix} V_{La,b,c\_\alpha} & V_{La,b,c\_\beta} \\ -V_{La,b,c\_\beta} & V_{La,b,c\_\alpha} \end{bmatrix} . \begin{bmatrix} i_{La,b,c\_\alpha} \\ i_{La,b,c\_\beta} \end{bmatrix} \quad (7)$$

$p_{La,b,c}$ and $q_{La,b,c}$ are load active and reactive powers per phase.

Instantaneous reactive and active powers have two components, i.e., mean (dc) and oscillating.

$$\begin{aligned} q_{La,b,c} &= q_{La,b,c\_dc} + \tilde{q}_{La,b,c} \\ p_{La,b,c} &= p_{La,b,c\_dc} + \tilde{p}_{La,b,c} \end{aligned} \quad (8)$$

p_{La,b,c_dc}, q_{La,b,c_dc} and $\tilde{p}_{La,b,c}$, $\tilde{q}_{La,b,c}$ are the dc and oscillating components of the load active and reactive powers per phase respectively.

The fundamental harmonic positive sequence component of the load, the dc component, and all load harmonics constitute the oscillating component of the active and reactive instantaneous power for each phase. The proposed converter aims to fully compensate for the load. Therefore, if the grid-interface converter can provide the oscillating active power of the load along with the total reactive power of the load, harmonic and reactive power compensation of the load will be achieved from the grid's point of view.

In addition, the unbalanced load power can be balanced by properly distributing it between the inverter and the grid. In this way, the total load seen by the grid is balanced. The three-phase dc component related to the active power of the unbalanced load can be obtained as follows:

$$p_{L\_dc} = p_{La\_dc} + p_{Lb\_dc} + p_{Lc\_dc} \quad (9)$$

where p_{L_dc} is the total three-phase dc component of the unbalanced load active power. Consequently, if it is assumed that the load is balanced, the dc component of the load active power consumption per phase will be obtained as follows:

$$p_{L_{ph}\_dc} = \frac{p_{L\_dc}}{3} \quad (10)$$

where $p_{L_{ph}\_dc}$ is the dc component of the balanced load active power for each phase.

Equation (10) and related concepts are used to determine the reference currents of the converter for load compensation. Besides transferring the PV-generated power to the grid, the PV-grid converter distributes the power among the phases so that the load reactive power and harmonics are compensated, and the grid load is balanced. Based on this, in the α-β frame, the currents that must be injected by the converter into the network/load are obtained as follows:

$$\begin{bmatrix} i_{Ca,b,c\_\alpha} \\ i_{Ca,b,c\_\beta} \end{bmatrix} = \begin{bmatrix} V_{La,b,c\_\alpha} & V_{La,b,c\_\beta} \\ -V_{La,b,c\_\beta} & V_{La,b,c\_\alpha} \end{bmatrix}^{-1} . \begin{bmatrix} p_{La,b,c} - \left(p_{L_{ph}\_dc} + p_{dclink}\right) + P_{pv\_mppt} \\ q_{La,b,c} \end{bmatrix} \quad (11)$$

i_{Ca,b,c_α} and i_{Ca,b,c_β} are the converter's reference currents in the α-β frame for each phase; $p_{La,b,c}$ and $q_{La,b,c}$ are the load active and reactive powers per phase; $p_{L_{ph}\_dc}$ is the reference power obtained by (10); P_{pv_mppt} is the maximum PV power obtained from the MPPT algorithm, and P_{dclink} denotes the active power that maintains the DC-link voltage at the voltage of maximum power (obtained from MPPT).

The perturb and observe (P&O) method is employed in the present study for MPPT. The P&O is known as the most widespread MPPT algorithm due to its easy implementation, simple control structure, and effectiveness. According to P&O, the PV output terminal voltage is periodically incremented or decremented, and the power values of the current and previous cycles are compared. With the variation of voltage and an increase (reduction) in power, the operating point is accordingly (oppositely) changed by the control system [23]. In a single-stage PV-grid interface inverter, the DC-link reference voltage is set to the value obtained from the MPPT for the PV system operating at maximum power. In

this method, with voltage and current sensors, the current power of the PV panels is calculated; then, the output power of the inverter is determined. Meanwhile, the DC link voltage must remain stable. The limitation in tracking speed by changing the step length and control period is effective in DC-link voltage stability. However, in rapid changes of radiation and temperature, the DC-link voltage stability cannot be assured. In order to stabilize the DC-link voltage in the single-stage PV-grid interface inverter, if the PV panel's output power decreases, the inverter's reference output power should be reset to the current output power of the PV. In other words, the input and output current of the DC-link should be balanced to maintain its voltage at the maximum power point, so that the tracking of the maximum power point is realized to absorb maximum energy. This is achieved in the proposed control strategy according to (11).

Fig. 2 presents the flowchart of an adapted P&O algorithm. Thus, according to (1) and (3), the three-phase reference currents of the converter are:

$$i_{Ca}^{*} = i_{Ca\_\alpha},\ i_{Cb}^{*} = i_{Cb\_\alpha},\ i_{Cc}^{*} = i_{Cc\_\alpha} \quad (12)$$

where i_{Ca}^{*}, i_{Cb}^{*}, and i_{Cc}^{*} are the reference currents of the converter for the a, b, and c phases respectively.

The block diagram of the reference current generation is shown in Fig. 3.

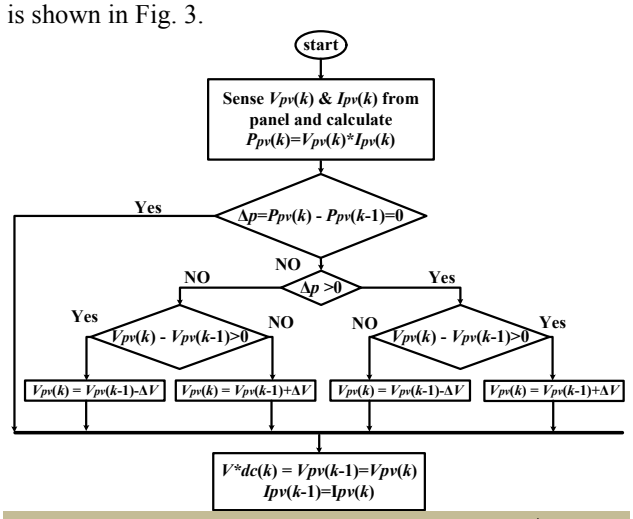

Fig. 2: Adapted P&O detection algorithm V_{dc}^{*}

Generally, a PV grid interface converter has two control loops. The outer loop determines the output current of the converter based on the control strategy. The inner loop modulates the output currents of the converter to meet the requirements of the waveform and phase. As mentioned, in single-stage PV grid interface converters, both loops are realized simultaneously in one power conversion stage. In this paper, based on the proposed control strategy, the output reference currents of the inverter are determined for the outer control loop, and in the inner control loop, pulse width modulation (PWM) is used to modulate the output currents of the inverter. According to the structure of the proposed inverter, this modulation is done separately for each phase.

In order to function without distorting the inverter controller to follow the reference currents, the voltage amplitude of the DC link must be greater than the voltage amplitude of each phase of the network (based on the topology of three single-phase H bridges). Considering that in the single-stage PV grid interface converter used in this paper, the DC link voltage is the same as the PV panels voltage, the minimum reference voltage for the DC link is considered to be the minimum amplitude of line-to-neutral voltage. This issue is included in the MPPT algorithm. Based on this, as stated in sectiontwo, one of the important points in choosing PV panels for the proposed grid interface converter is the range of PV voltage amplitude changes which should be within the permissible range of DC link voltage amplitude changes of the inverter. Based on this, the inverter topology used in this paper is very suitable for the low PV voltage amplitude range.

4. Simulation

In the present study, the proposed control method is evaluated for a single-stage PV-grid interface converter using the MATLAB/SIMULINK software while compensating for nonlinear and unbalanced loads in a four-wire three-phase distribution network. The simulated system is shown in Fig. 1. In this system, the PV unit is connected to the network by a single converter through isolated transformers in parallel with the load. Nonlinear and linear loads are combined to represent the load. A three-phase rectifier with a resistive dc load forms the nonlinear load. A set of resistive and inductive impedances is considered to be the linear load. The linear load draws unbalanced active and reactive power from the grid. Moreover, the switching harmonics are suppressed by using a passive filter. Table 1 shows the simulation parameters.

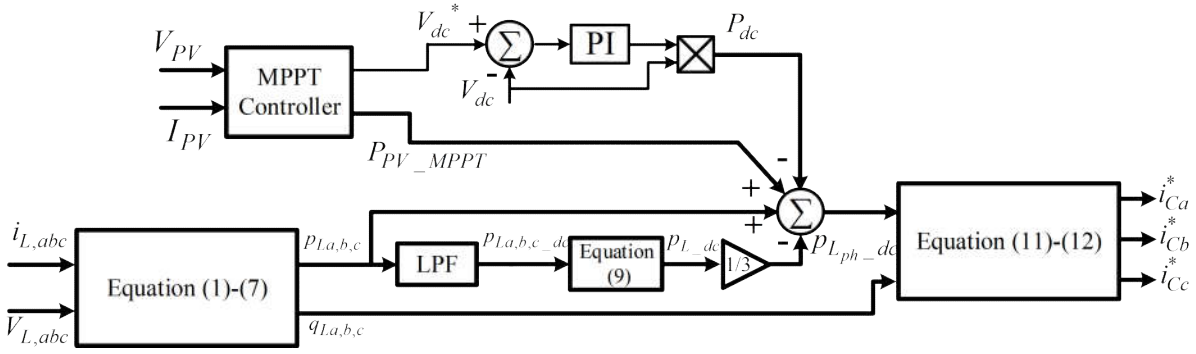

Fig. 3: Block diagram for reference current generation

Table 1: Simulation parameter values

Network parameters	$V_{rms\_phase}=220V, f=50Hz,$ $L=100\mu H, R=0.01\Omega$
Nonlinear and unbalanced load	Nonlinear load: Resistor loaded by diode rectifier, $R_r=55\Omega$
	Unbalanced load: $R_a=20\Omega, R_b=60\Omega,$ $L_b=1mH, R_c=25\Omega$
DC/AC inverter	Transformer turn ratio=1; $V_{dc\_min}=330V, C_{dc}=500\mu F,$ $f_{sw}=10kHz$
Passive filter	$L=4mH$

Fig. 4 shows the dynamic model of the solar cells. The internal resistance is denoted by the series resistance R_S, and R_{sh} is the parallel resistance that depends inversely on the ground leakage current. The PV arrays are made of parallel-connected single-module strings. Each string contains 15 series-connected modules, to obtain the desired rated power at the suitable voltage [15].

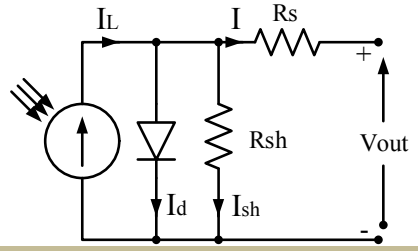

Fig. 4: Equivalent circuit of a PV cell

Table 2 presents the PV unit parameters. Voltage-power and current-voltage characteristic curves of PV panels at various solar irradiances and temperatures are shown in Fig. 5. The MPPT algorithm tracks the MPP, which is at a specific voltage as shown in Fig. 5.

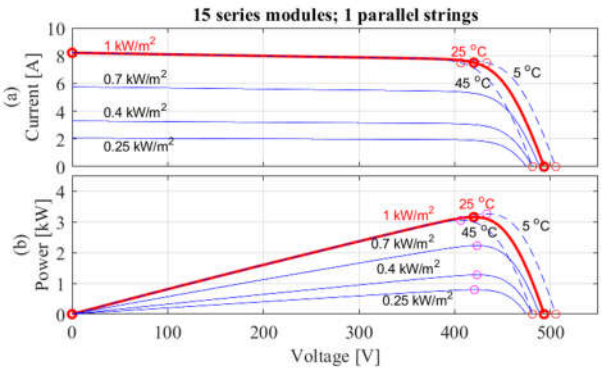

Fig. 5: (a) Current-voltage and (b) power-voltage characteristics of PV panel at different irradiations and temperatures

4.1. Simulation Results

The simulation results of the system in Fig. 1 are shown in Fig. 6 based on the parameter values in Table 1. The inverter starts to operate at 0.07 s to improve its performance and exhibit its capabilities. The grid voltage is illustrated in Fig. 6(a).

The three-phase currents of the load are shown in Fig. 6(b). These currents are unbalanced and non-sinusoidal. The average total harmonic distortion (THD) of the phases is approximately 18%. Fig. 6(c) and (d) show the three-phase compensation and grid currents respectively. As shown, the load harmonics and imbalance in the grid currents cannot be observed after 0.07 s, that is, when the compensator is operated. This means that current harmonics and imbalance are compensated. The average THD of the phases is approximately 2.2%. Under this condition, the power consumed by the load is larger than the PV generation. Therefore, both the PV and grid supply the load, and a smaller grid current is required compared to the time when the converter was not installed.

Table 2: PV panel parameters

Array data		Module data			
Parallel string	1				
Series-connected modules per string	15	Temperature coefficient of Voc [%/deg.C]	-0.123	Temperature coefficient of Isc (%/deg.C)	0.0032
		MPP voltage Vmp [V]	28	MPP current Imp [A]	7.5
		Open circuit voltage Voc [V]	32.9	Short-circuit current Isc [A]	8.21
		Maximum Power [W]	210	Cells per module (Ncell)	54
		Parameters of model			
		Light-generated current IL [A]	8.2431	Shunt resistance Rsh [ohms]	59.408
		Diode saturation current [A]	8.917e-16	Series resistance Rs [ohms]	0.23963

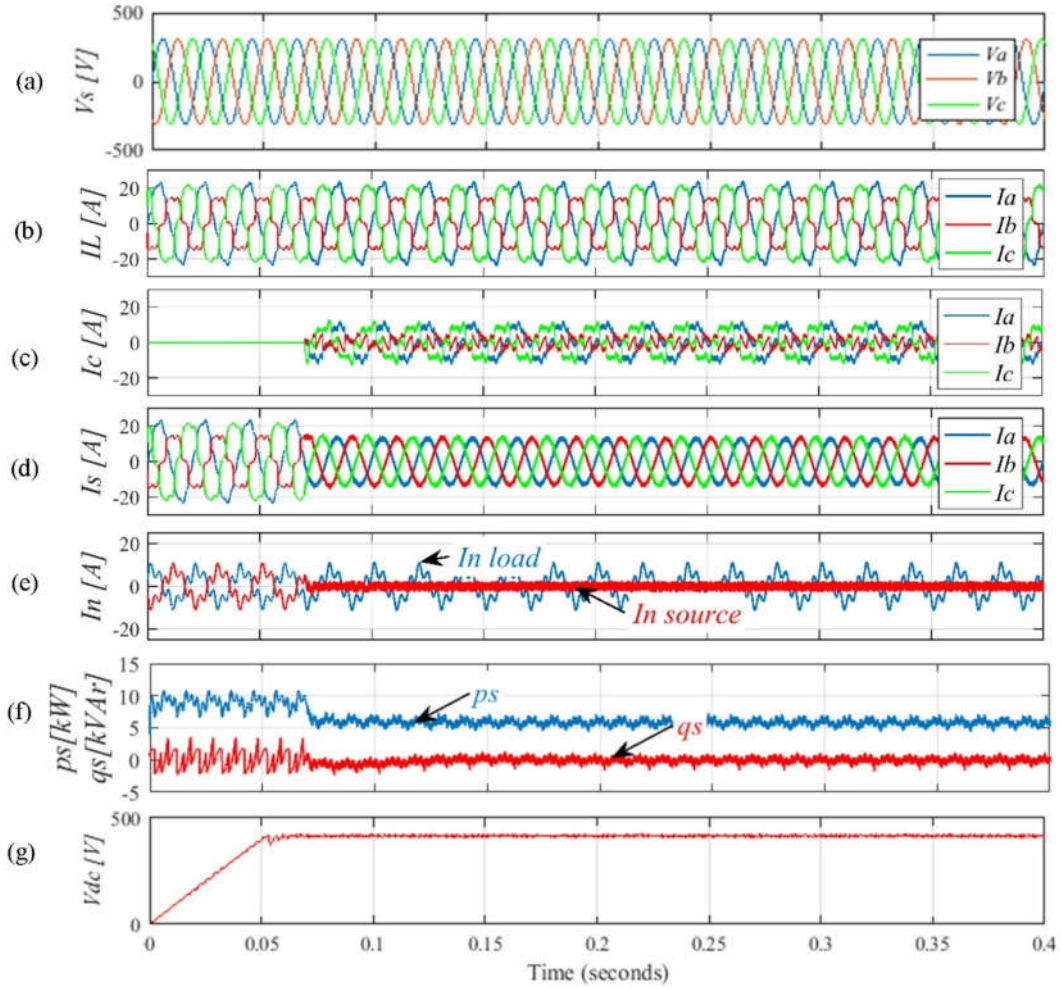

Fig. 6: Simulation results of the proposed structure; (a) phase voltage of source, (b) load current, (c) compensation current, (d) source current, (e) source and load neutral current, (f) DC-link voltage, and (g) three-phase reactive and active power of source

The load and source neutral currents are shown in Fig. 6(e). According to this figure, the unbalanced load current is properly offset, and it seems that the load is balanced from the grid's point of view. The total three-phase active and reactive power of the grid is shown in Fig. 6(f). According to this figure, the three-phase reactive power tends to zero when the inverter starts to operate. Therefore, the reactive power is offset as aimed. The grid active power decreases by injecting PV power into the load, so the presence of the PV system leads to desirable results.

Fig. 6(g) shows the DC voltage of the PV panel and the converter. The DC link voltage is around 420 V, which is at MPP. From Fig. 6, the proposed structure and the control strategy can effectively perform the PV MPPT, transmit the PV power to the load and grid, and achieve the compensation objectives.

To demonstrate better and compare the performance results of the proposed PV-grid interface converter in improving the grid power quality, the simulation results of the PV-grid interface converter are presented in Table 3. The THD of the three-phase currents, the RMS of the three-phase currents, and the unbalance factor (UF) [24] of the currents for the two cases of "with" and "without" the PV-grid interface converter are presented in Table 3. The value of UF is expressed as the ratio of maximum deviation from the average three-phase current to the average three-phase current in percent.

Table 3: Results of comparison between the proposed and conventional methods

		THD%		Three-phase currents (RMS) [A]	UF%
Load parameters (No compensation)	A:	9.77	A:	15.85	22.93
	B:	20.56	B:	11.08	
	C:	15.9	C:	16.25	
Proposed method	A:	2.19	A:	9.19	1.12
	B:	2.20	B:	9.28	
	C:	2.23	C:	9.39	

4.2. Performance of PV-grid Interface Converter with Variations in Solar Radiation and Temperature

This section evaluates the effect of variations in solar radiation and temperature on the performance of the converter and the proposed control scheme. Fig. 7 shows the simulation results for the system in Fig. 1 based on the parameter values in Table 1 with variations in solar radiation in the range of 0.4-1.4 s and variations in temperature in the range of 2-3.5 s.

The variations of solar radiation and temperature are shown in Fig. 7(a) and 7(b) respectively. According to Fig. 7 (c), the generated PV power changes with variations in solar radiation and temperature. Fig. 7 (d) illustrates the grid voltage. The non-sinusoidal and unbalanced three-phase load currents are shown in Fig. 7 (e). The three-phase compensation and grid currents are shown in Figs. 7 (f) and 7 (g) respectively. The grid current contains no large imbalance and harmonics resulting from the load current. Furthermore, the response of the proposed control scheme to fast variations in solar radiation and temperature is flawless. Load consumption is greater than the generation of the PV, and both the grid

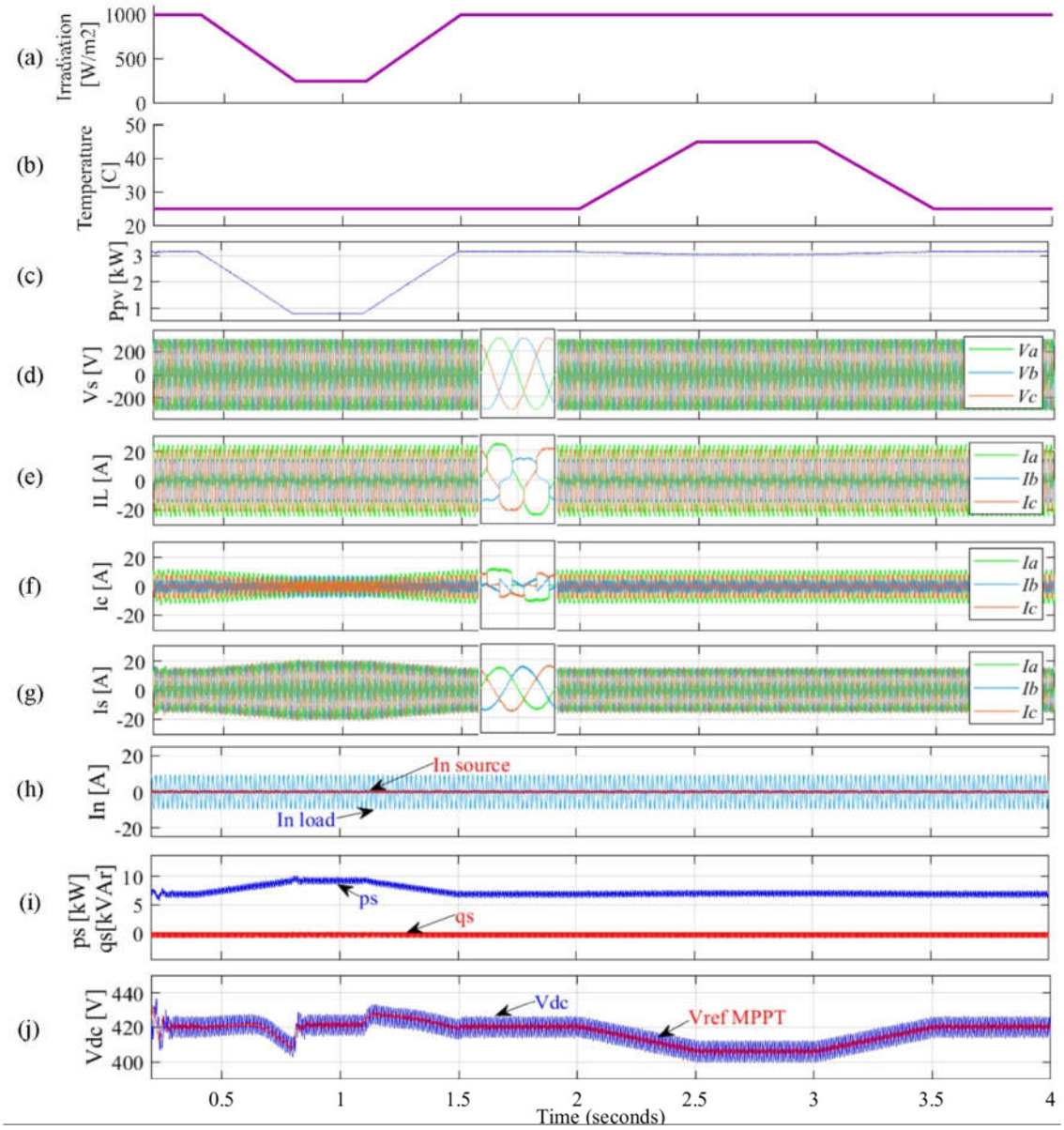

Fig. 7: Simulation results for the variations in solar radiation and temperature; (a) Radiation, (b) temperature, (c) PV power, (d) source voltage, (e) load current, (f) compensator current, (g) source current, (h) source and load neutral current, (i) three-phase reactive and active power of source, and (j) PV DC voltage

and PV system supply the load. A decrease in the PV generation during the interval 0.4-1.4 s and 2-3.5 s reduces the contribution of PV; therefore, the contribution of load supply by the grid increases, and so does the network current. This issue is more visible in the changes in the sun's radiation.

The neutral load and grid currents are shown in Fig. 7 (h). The load current imbalance during temperature and solar radiation variations is properly compensated by the proposed control scheme. The total values of three-phase active and reactive grid power are illustrated in Fig. 7(i). According to this figure, the three-phase reactive power is approximately zero over the investigated temperature and solar radiation range. Accordingly, the objective of reactive power compensation is achieved. More power is supplied by the grid to the load because of the reduction in PV power. The PV DC voltage is shown in Fig. 7(j). According to Fig. 5 and Fig. 7(j), it can be seen that the DC-link voltage follows the MPP voltage. Also, according to the PV power changes in Fig. 7(c) and the network power changes in Fig. 7(i), it can be concluded that MPPT has been achieved.

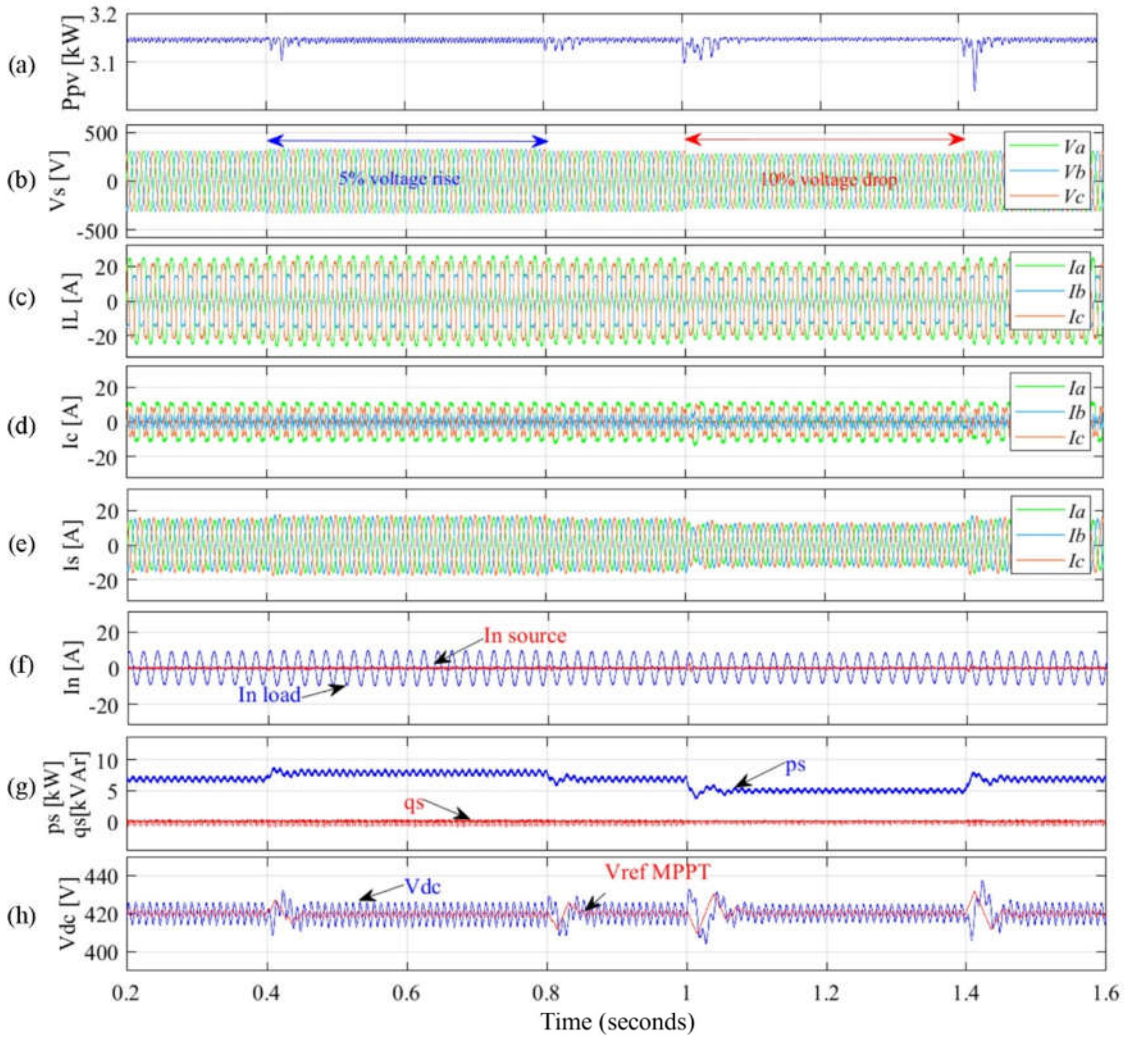

Fig. 8: Simulation results in the conditions of network voltage drop and rise; (a) PV power, (b) source voltage, (c) load current, (d) compensation current, (e) source current, (f) source and load neutral current, (g) three-phase reactive and active power of source, (h) PV DC voltage

4.3. Performance of PV-Grid Interface Converter in Grid Voltage Drop and Rise

According to the characteristics of the power distribution network, the network voltage is not always constant. With load changes, the network voltage may increase or decrease. According to the National Electrical Code, voltage variations in power distribution networks must be limited between 5% for voltage rise and -10% for voltage drop. Based on this instruction, in this section, the performance of the converter and the proposed control

scheme in the network's voltage drop and rise is evaluated.

Fig. 8 shows the simulation results for the system in Fig. 1 based on the parameter values in Table 1 with a voltage rise in the time range of 0.4 to 0.8 seconds by 5% and a voltage drop in the time range of 1 to 1.4 seconds by 10%. Fig. 8(a) shows the power generated by PV. As seen, during the rise and drop of the grid voltage, the PV continues to generate power in MPP. The per-phase grid voltage is shown in Fig. 8(b). According to the figure, a 5% voltage rise occurred in the interval of 0.4-0.8 seconds, and the 10% voltage drop occurred in the interval of 1-1.4 seconds. Fig. 8(c) illustrates the three phases current of the load. Changes in load current amplitude are caused by variations in grid voltage amplitude. Fig. 7(d) and 7(e) show the three-phase compensation and grid currents respectively. As seen, the load compensation is properly performed by the converter even during the grid voltage drop and rise. The neutral load and grid currents are shown in Fig. 7(f). According to Fig. 7(f) the neutral load current is properly compensated by the proposed converter. The three-phase active and reactive grid power are illustrated in Fig. 7(g). According to this figure, the objective of reactive power compensation has been achieved. Fig. 7(h) shows the PV DC voltage. According to Figure, the DC-link voltage follows the MPP voltage. Therefore, according to the PV power in Fig. 7(a) and the PV voltage in Fig. 7(h), MPP has been tracked.

5. Conclusion

In the present study, a single-stage PV-grid interface inverter along with its control strategy, usingthe instantaneous power theory, is proposed. The proposed method was evaluated under unbalanced nonlinear loads. MATLAB/SIMULINK was used to validate the proposed method in a three-phase, four-wire distribution system.

According to the simulation results, the proposed method can effectively eliminate current harmonics, balance load, correct power factor, and improve network capacity utilization.

The implemented structure consisted of only one DC/AC converter. The DC/AC converter and its control strategy had the following features: PV MPPT, reactive power/unbalanced load compensation, load harmonic elimination, and PV power injection into the grid and load. The advantages of the proposed structure and its control strategy are its practical implementability and a reduction in equipment costs, compared with two-stage structures.

References

[1] Hussein, A., Chen, X., Alharbi, M., Pise, A. A., Batarseh, I., "*Design of a Grid-Tie Photovoltaic System with a Controlled Total Harmonic Distortion and Tri Maximum Power Point Tracking*", IEEE Transactions on Power Electronics, Vol. 35, No. 5, pp. 4780-4790, May 2020., doi:10.1109/TPEL.2019.2946586.

[2] Horoufiany, M., Ghandehari, R., "*Economic Evaluation of the Installed PV Arrays in a Certain Area of Solar Fields by the Deployment of the Fixed Reconfiguration Method*", Journal of Energy Engineering & Management (JEM), Vol. 8, No. 5, pp. 2-11, 2018., (In Persian), doi:10.22052/8.1.2.

[3] Xia, Z., Liu, Z., Guerrero, J. M., "*Multi-Objective Optimal Model Predictive Control for Three-Level ANPC Grid-Connected Inverter*", IEEE Access, Vol. 8, pp. 59590-59598, 2020., doi:10.1109/ACCESS.2020.2981996.

[4] Ala'a, M., Qadourah, J.A., Alrwashdeh, S.S., Qatlama, Z., Alddibs, E., Noor, M., "*Energy performance and economics assessments of a photovoltaic-heat pump system*", Results in Engineering, Vol. 13, 2022., doi:10.1016/j.rineng.2021.100324.

[5] Reveles-Miranda, M., Flota-Bañuelos, M., Chan-Puc, F., Ramirez-Rivera, V., Pacheco-Catalán, D., "*A Hybrid Control Technique for Harmonic Elimination, Power Factor Correction, and Night Operation of a Grid-Connected PV Inverter",* IEEE Journal of Photovoltaics, Vol. 10, No. 2, pp. 664-675, March 2020., doi:10.1109/JPHOTOV.2019.2961600.

[6] Mousazadeh Mousavi, S.Y., Jalilian, A., Savaghebi, M., Guerrero, J.M., "*Power quality enhancement and power management of a multifunctional interfacing inverter for PV and battery energy storage system*", International Transactions on Electrical Energy Systems, Vol. 28, No. 12, 2018., doi:10.1002/etep.2643.

[7] Kalair, A., Abas, N., Kalair, A.R., Saleem, Z., Khan, N.,

"*Review of harmonic analysis, modeling and mitigation techniques*", Renewable and Sustainable Energy Reviews, Vol. 78, pp. 1152–1187, April 2017., doi:10.1016/j.rser.2017.04.121.

[8] Ansari, M. R., Mousavi Ghahfarokhi, M. S., Safaee, S., "*Power Quality Improvement in a Steel Plant by an Optimized Shunt Active Power Filter Based on Developed P-Q Theory*", Journal Energy Engineering & Management (JEM), Vol. 11, No. 3, pp. 78-91, 2021., (In Persian) doi:10.22.52/11.3.3.

[9] Afkar, H., Shamsi Nejad, M. A., Ebadian, M., "*A grid-connected PV inverter with compensation of load active and reactive power imbalance for distribution networks*", Iranian Journal of Electrical & Electronic Engineering, Vol. 12, No. 2, pp. 168-176, Jun. 2016., doi:10.22068/IJEEE.12.2.168.

[10] Sivaraman, P., Sharmeela, C., Power Quality in Modern Power Systems, Academic Press, 2020.

[11] Md Rafi, F. H., Hossain, M. J., Town, G., Lu, J., "*Smart Voltage-Source Inverters With a Novel Approach to Enhance Neutral-Current Compensation*", IEEE Transactions on Industrial Electronics, Vol. 66, No. 5, pp. 3518-3529, May 2019., doi:10.1109/TIE.2018.2856188.

[12] Li D., Wang, T., Pan, W., Ding, X., Gong, J., "*A comprehensive review of improving power quality using active power filters*", Electric Power Systems Research, Vol. 199, pp.107389, 2021., doi:10.1016/j.epsr.2021.107389.

[13] Paulo Bonaldo, J., Lessa Tofoli, F., Vitor Arantes, R., Morales-Paredes, H., "*Comparative analysis of techniques for the limitation of compensation currents in multifunctional grid-tied inverters*", International Journal of Electrical Power & Energy Systems, Vol. 126, 2021., doi:10.1016/j.ijepes.2020.106574.

[14] Liang, X., Andalib -Bin- Karim, C., "*Harmonics and Mitigation Techniques Through Advanced Control in Grid-Connected Renewable Energy Sources: A Review*", IEEE Transactions on Industry Applications, Vol. 54, No. 4, pp. 3100-3111, July-Aug. 2018., doi:10.1109/TIA.2018.2823680.

[15] Patel, N., Gupta, N., Bansal, R.C., "*Combined active power sharing and grid current distortion enhancement-based approach for grid-connected multifunctional photovoltaic inverter*", Transactions on Electrical Energy Systems, Vol. 30, No. 3, pp. 1–27, 2020., doi:10.1002/2050-7038.12236.

[16] Babu P, N., Guerrero, J. M., Siano, P., Peesapati, R., Panda, G., "*An Improved Adaptive Control Strategy in Grid-Tied PV System With Active Power Filter for Power Quality Enhancement*", IEEE Systems Journal, Vol. 15, No. 2, pp. 2859-2870, June 2021., doi:10.1109/JSYST.2020.2985164.

[17] Mantilla, M.A., Petit, J.F., Ord´o˜nez, G., "*Control of multi-functional grid-connected PV systems with load compensation under distorted and unbalanced grid voltages*", Electric Power Systems Research, Vol. 192, October 2021., doi:10.1016/j.epsr.2020.106918.

[18] Boukezata, B., Gaubert, J.P., Chaoui, A., Hachemi, M., "*Predictive current control in multifunctional grid connected inverter interfaced by PV system*", Solar Energy, Vol. 139, pp. 130–141, 2016., doi:10.1016/j.solener.2016.09.029.

[19] Lin, F. -J., Lu, K. -C., Yang, B. -H., "*Recurrent Fuzzy Cerebellar Model Articulation Neural Network Based Power Control of a Single-Stage Three-Phase Grid-Connected Photovoltaic System During Grid Faults*", IEEE Transactions on Industrial Electronics, Vol. 64, No. 2, pp. 1258-1268, Feb. 2017., doi:10.1109/TIE.2016.2618882.

[20] Guo, B., *et al*., "*optimization design and control of single-stage single-phase PV inverters for MPPT improvement*", IEEE Transactions on Power Electronics, Vol. 35, No. 12, pp. 13000-13016, Dec. 2020., doi:10.1109/TPEL.2020.2990923.

[21] Zeb, K., *et al*., "*A comprehensive review on inverter topologies and control strategies for grid connected photovoltaic system*", Renewable and Sustainable Energy Reviews, Vol. 94, pp. 1120-1141, 2018., doi:10.1016/j.rser.2018.06.053.

[22] Bajaj, M., Singh, A. K., "*Grid integrated renewable DG systems: A review of power quality challenges and state-of-the-art mitigation techniques*", International Journal of Energy Research, Vol. 44, No. 1, pp. 26-69, 2020., doi:10.1002/er.4847.

[23] Belfedhal, S.A., Berkouk, E.M., Messlem, Y., "*Analysis of grid connected hybrid renewable energy system*", Journal of Renewable and Sustainable Energy, Vol. 11, No. 1, 2019., doi:10.1063/1.5054869.

[24] Mohammadi, H. R., Hajiakbari Fini, M., "*A Novel Control Strategy for Shunt Active Power Filter in Three-phase Four-wire System to Compensate Harmonics, Unbalance and Reactive Power*", Journal of Energy Engineering & Management (JEM), Vol. 4, No. 2, pp. 2-9, 2014., (In Persian)